marine technology SOCIETY
Journal
The International, Interdisciplinary Society Devoted to Ocean and Marine Engineering, Science, and Policy
Volume 52 Number 6 November/December 2018

Advancing Oil Spill Technology: Beyond the Horizon

TECHNICAL NOTE

Infrared Polarimetric Sensing of Oil on Water

AUTHORS

David B. Chenault
Justin P. Vaden
Polaris Sensor Technologies, Inc., Huntsville, Alabama

Douglas A. Mitchell
Erik D. Demicco
ExxonMobil Upstream Research Company, Spring, Texas

ABSTRACT

Infrared polarimetry for surface spill detection is an emerging sensing modality shown to significantly enhance contrast in situations where conventional thermal imaging cannot detect a spill. Imaging of the polarization signatures of oil and water in a scene can lead to enhanced understanding, particularly when the materials in a scene are at thermal equilibrium. Testing at Ohmsett has shown good performance with multiple types of crude oil, diesel fuel, and kerosene in several different viewing geometries. Over the course of two separate tests at Ohmsett, recoverable oil was detected during day and night, in calm water and in waves, when puddled on sand and rocks, with and without dispersant, on the surface after subsurface releases, and for fresh, aged, and emulsified oil. In-situ testing has confirmed these capabilities. This new remote sensing capability offers the promise of automated detection of oil spills and leaks for routine monitoring and accident response with the added benefit of continued monitoring at night. The camera has a small form factor that is compatible with all types of platforms including small drones. Polaris Sensor Technologies has tested this technology extensively at the Ohmsett Test Facility with several opportunistic tests in the Gulf of Mexico and near Santa Barbara, CA, with an emphasis on finding the limits of performance. In this paper, we describe the instrumentation and the test results in both controlled and uncontrolled conditions.

Keywords: oil spill detection, remote sensing, surface spill, environmental monitoring, infrared polarization

Introduction

Technologies for detecting, monitoring, and tracking oil spills have advanced significantly over the last 10 years. However, most of these methods are point detection approaches that limit the scope of detected area or detect a minimum thickness that is often higher than what is recoverable. There is a need for remote sensing capability that covers larger areas and addresses oil thicknesses that are recoverable. The ability to detect and track oil over a wide area is necessary to make the most efficient use of response resources. For relatively small spills, the response is heavily dependent on being able to locate the spill based on sporadic, sometimes nonspecific reports, and to determine its size. With larger spills, a coordinated response team may be continually on site, but recovery operations are often limited to daylight hours. Updates are then required on the spill location in the morning before recovery operations can begin, often causing hours of delay in oil recovery or mitigation (Svejkovsky et al., 2016). Infrared imaging is used in some cases; however, the thermal contrast between the oil and the water background is typically small particularly at night and is further confounded by wave action. The ability for personnel to quickly and easily detect oil on water is clearly needed for an appropriate, consistent, and cost-effective response (Svejkovsky et al., 2016). The potential to automatically perform the same function could be a boon for oil responders and provide the opportunity for regular monitoring around drilling operations and facilities, transfer points, ports, and harbors.

In 2015, an oil pipeline near Santa Barbara, CA, ruptured, resulting in a spill into the Santa Barbara channel. An aerial survey of the oil spill with an infrared polarimeter developed by Polaris Sensor Technologies resulted in significant improvement of oil detection over conventional thermal cameras. Furthermore, the polarization signature was immune to false positives such as kelp, sun glint, and clutter from the shoreline. With partial support from ExxonMobil Upstream Research Company, we subsequently had the opportunity to test an infrared polarimeter at Ohmsett, the National Oil Spill Response Research & Renewable Energy Test Facility in northeast New Jersey. This test facility, managed by the U.S. Department of Interior's Bureau of Safety and Environmental Enforcement, provides independent, objective performance testing of oil spill response equipment on a large scale and in as realistic environment as possible. A Polaris Pyxis® Long Wave Infrared (LWIR) 640 infrared

imaging polarimeter recorded a number of controlled spills to test its detection performance as a function of time of day and angle, oil type and thickness, and of the evolution and motion of several oil types in both calm water and in waves. In all cases, the infrared polarimetric data showed superior detection over that of thermal infrared alone and enabled detection of even small amounts of oil on the water's surface throughout the night and in situations when the thermal imagery showed no contrast.

A subsequent test at Ohmsett and *in situ* tests in the Gulf of Mexico confirm the performance of the Pyxis camera for oil spill detection. Testing to date has determined that the minimum detectable thickness lies in the range of 10–100 µm, which corresponds to metallic on the Bonn appearance scale. The detection performance is robust with respect to variables such as time of day, presence of waves, different types of hydrocarbons, and with fresh and emulsified oil.

Similar measurements in the past required large scientific instruments not readily applicable for hand-held use. Recent development of uncooled, microbolometer infrared sensors has led to a significant reduction in size, weight, power, and cost for such sensors. The Pyxis infrared polarimetric camera incorporates a microfilter polarizing array mounted in close contact to the microbolometer focal plane array (FPA). This highly integrated approach for optical filtering is the enabling technology for achieving the small size.

The Pyxis passively measures not only the conventional thermal intensity of a scene but also the polarization magnitude and orientation of the plane of polarization. In general, the measurement of the parameters of the optical polarization ellipse gives details in a scene that are not readily apparent when using conventional thermal imagers alone. The strength and orientation of an infrared polarimetric signal relies on material parameters, orientation, surface roughness, aspect angle to the sensor, down-welling sky radiance, and background radiance reflecting from the objects in the scene. Often, the polarization signature of objects with different material properties is different than that of the surrounding background. Most importantly, that difference is often present even when the intensity signature of the object is in thermal equilibrium with the background (Felton et al., 2010a, 2010b). In other words, the materials or surfaces can be completely invisible in the standard intensity image, while at the same time exhibiting a strong polarimetric signature. Furthermore, the fact that the polarization signal is based on emission, the polarization signal is available for day/night operations. It is this capability to provide polarization contrast resulting from material differences that we are exploiting here for oil on water detection (Chenault et al., 2016; Chenault & Vaden, 2018).

In this paper, we describe the technology, the hardware and software, and the tests at Ohmsett and in the Gulf of Mexico.

Technology Overview

The technology underlying the Pyxis sensor exploits the polarization of light in our environment. Polarization is one of the three independent quantities in electromagnetic radiation along with magnitude and frequency (wavelength). However, these three quantities are independent of each other so that two beams of light with the same intensity and wavelength (or spectral distribution) can have very different polarization states. When ambient illumination is reflected off an object, the reflected light can become polarized. Likewise, in the thermal infrared, light can be polarized in both emission and reflection. An imaging polarimeter measures these polarization states and provides additional information that exploits the polarization differences in the scene that are frequently different from the broadband intensity. The magnitude of the polarization signature in a scene depends on the angles of the surface normals relative to the sensor look angle and the surface optical characteristics.

At certain times of day, the apparent temperature of the oil can match the apparent temperature of the surrounding background, and the object can be very difficult to see in the thermal image (Allik et al., 2016; Myhr et al., 2018). These events are referred to as thermal cross-over periods and typically occur twice daily, once after sunrise and again after sunset, but can occur at other times depending on ambient conditions. Polarization excels in these situations. It is important to note that, although polarization measurements do not require intensity or thermal contrast, any thermal signature that is present is also detected. LWIR thermal and polarization imaging is combined in a single camera so that together the camera provides advantages over conventional thermal imagers in detection applications.

The specific configuration of an imaging polarimeter depends on a number of design requirements, which, in turn, are dependent on the application and the state-of-the-art technologies available to meet those requirements. The physical configuration can be

broken into categories according to the optical path and layout of the electro optical components (Tyo et al., 2006). There are five primary configurations for imaging polarimeters: rotating element or division of time, division of amplitude, division of aperture, micro-optic or division of focal plane (DoFP), and channeled instruments. For scenarios where the scene is dynamic with wave action and the sensor and/or the sensor platform may be moving, the DoFP approach is the best choice and is the one implemented in the Pyxis handheld polarimeter.

Recent advances in micro-optics manufacturing have allowed the integration of micro-optical polarization elements directly onto a FPA, thus creating a "DoFP" polarimeter. In this configuration, pixelated linear polarization elements are attached intimately to the FPA. Systems operating in the visible, Short Wave Infrared (SWIR), and LWIR wavebands have been built using this technology. Most DoFP systems use interlaced polarization super-pixels to calculate the polarization parameters at interpolation points on the FPA. It should be noted that the intensity information is still collected at the full resolution of the FPA. DoFP systems have some significant advantages. All polarization measurements are made simultaneously for every pixel in the scene, and it uses a single FPA with no added complications to the optical train. The architecture is very similar to commercial color cameras that use a Bayer color filter overlay on the FPA.

Data fusion is possible, exploiting both the thermal and polarization data products. The imagery can be viewed independently or fused images can be formed from combinations. Data fusion captures all the information and displays it in a single image, giving the operator a more intuitive view of the scene. In the fused image, the unpolarized thermal image is displayed as normal grayscale. The polarization is displayed in color from a user-defined threshold. When a pixel exceeds that threshold, the pixel is colored based on the linear polarization. For oil on water detection, this fusing capability tends to highlight the oil with color while still providing context through the gray scale infrared image information.

Sensor Description

The measurement of polarimetric phenomenology requires capturing images with polarization filters. The approach used here is based on the DoFP polarimetric architecture for imaging polarimeters. For infrared applications, the pixelated polarizer array uses an infrared transmitting substrate. A metal layer is deposited on the substrate. and then the wire grid pattern is etched in to the metal layer using standard semiconductor processing techniques creating the wire grid pattern. The polarizers are oriented at 0° and 90°, and 45°and 135°. The pixels in different polarization states in a DoFP imaging polarimeter are combined to determine the polarization state of each super-pixel. A super-pixel is composed of a 2 × 2 array of pixels. The measured incident polarization state is determined based on a weighted sum of interpolated pixels. It is important to note that, through this interpolation, both thermal and polarization images are captured at the full resolution of the array. In addition, because the polarization sensitivity is integrated on the FPA, no additional optics are added to the optical train and the system is no larger and is equally as rugged as a conventional camera.

Two models of Pyxis are shown in Figure 1. The Pyxis 640 LWIR-G model on the left outputs unprocessed digital data through a Gigabit Ethernet cable for processing on a laptop or tablet. On the right, the Pyxis 640-GR case and cord are configured for IP67 environmental ruggedization but is otherwise operationally identical to the -G version. Mounting points on the bottom can be used to mount the sensor to a tripod or handle, or to a drone gimbal.

All versions of the camera interface to a computer (or tablet) and use the Pyxis Vision Science (PVS) software framework developed by Polaris for commercial applications. PVS provides the ability to control the sensor, view the raw and processed sensor data, and record data. Note that the user interface provides a suite of standard color palettes, as well as toolbar

FIGURE 1

The Pyxis 640 LWIR-G and the Ruggedized Pyxis 640 LWIR-GR with Gigabit Ethernet interfaces.

buttons for selecting standard output imagery products. PVS gives the operator easy access to intensity data (temperature and radiance), polarimetric data, and fused data products (eTherm). The user can measure the value of a specific pixel or create a histogram or strip chart that displays the values for regions of interest within the image. PVS provides a full suite of options for recording raw data ranging from a single snapshot to periodic sequence recording creating time-lapse videos.

Ohmsett Testing

In July of 2016, Polaris participated in a week of oil spill detection tests at Ohmsett sponsored in part by the ExxonMobil Upstream Research Company, an ExxonMobil subsidiary that engages in research and development of technology for exploration, development, production, and gas commercialization. The test matrix consisted of 2 days of testing in a small, 1,000-gallon "fast tank" placed on the deck of the larger facility and then 2.5 days of testing in the large 2-million-gallon tank. The test objectives were to determine the effectiveness of infrared polarimetric imaging through the use of the Pyxis camera for the detection of oil on water compared to standard thermal imaging. Additionally, sensitivity of the technique relative to oil thickness, look angle, and ambient temperature changes, time of day, and wave action was evaluated.

During the fast tank testing, initial polarimetric and thermal data were collected on oil samples of known thicknesses of oil. Overnight, time-lapse imagery was collected to directly compare polarimetric and thermal response as the oil and water temperatures varied due to solar loading and night time radiative cooling. Angle-dependent data were collected by varying the look angle relative to the tank. Understanding of the angle sensitivity is important for optimizing placement of the sensor when deployed on ships, platforms, or unmanned aerial systems. Figure 2 shows the fast tank placed on the deck next to the large tank and the oil-containing bins with the Pyxis camera mounted on a man lift.

Figure 3 shows a sequence of the image data from the visible camera (left), the thermal output from the Pyxis camera (center), and the polarimetric image from the Pyxis camera (right). The view is roughly eastward looking with a down-look angle of about 30°. One second (30 frames) of this imagery was collected every 10 min from 3 pm on July 26, 2016 until 9 am the next morning. The time of the imagery shown in the figure is in the upper left corner of each row. The visible image shown at 21:27 is dark because there was no ambient illumination of the scene. Underneath these images is a time-correlated plot of the contrast ratio (CR) of the polarimetric and thermal measurements of each bin relative to the water background where the yellow vertical lines are placed at the appropriate time stamp. A variant of the *T*-test contrast metric was used here where the oil is denoted by *O*, the water background is denoted by *B,* thermal data is denoted by subscript T and polarization data is denoted by subscript P. The CRs for the thermal data (CR_T) and for the polarization data (CR_P) are then

$$CR_T = \frac{|O_T - B_T|}{6\sigma_T} \qquad CR_P = \frac{|O_P - B_P|}{6\sigma_P}$$

where the quantities are the mean of regions of interest chosen in the oil and water portions of the image and σ is the spatial standard deviation of each image. The top two lines in the plot show the polarimetric CR for the left bin (thicker oil, blue or darker gray) and right bin (thinner oil, orange or lighter gray). The bottom two lines in the plot show the thermal CR for the left bin (thicker oil, green or lighter gray) and right bin (thinner oil, red or darker gray).

The results from time-lapse overnight tests are important for several reasons. First, the ability to detect and track an oil spill in darkness could significantly increase the effectiveness and efficiency of response to a spill. This ability would also enable

FIGURE 2

"Fast tank" test setup for thickness, angle, and overnight testing. The view on the right shows a close up of the bins viewed by the sensor placed on the man lift. The bin on the left was filled with water and 1,000 ml of oil, resulting in an oil thickness of 5 mm, and the bin on the right was filled with water and 100 ml of oil, giving a thickness of 0.5 mm. The water level in the fast tank was just below that of the lip of the bin to keep a fairly pristine water background for comparison.

FIGURE 3

Time lapse, overnight imagery from the fast tank testing.

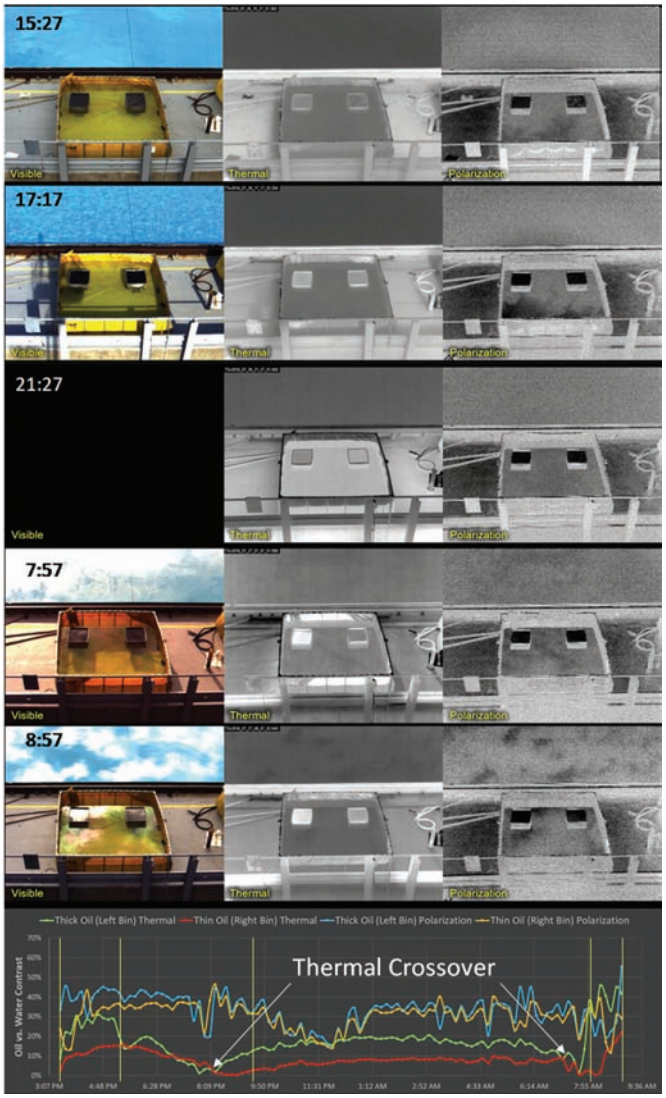

monitoring around drilling operations, transfer points, and ports and harbors and enable spill detection at the earliest possible time. Second, thermal cross-over events resulting from changes in apparent temperature of the oil relative to the water creates periods when the oil and water are in thermal equilibrium, and therefore, the oil is essentially invisible in thermal imagery. These cross-over events typically happen several hours after sunset and sunrise.

Although the time-lapse data shows good quantitative performance, it was desirable to perform testing in the large tank at Ohmsett to minimize nonwater background and to see the effect of waves on the polarimetric signature. Two and half days of testing provided the opportunity to look at the uncontrolled spreading of diesel fuel and two types of oil in both breaking and nonbreaking waves and any apparent changes when the sensor was moving along the tank. Figure 4 shows the mounting location on the bridge tower and the view of the tank from the sensor location. The sensor was also mounted in front of the window of the cab on the bridge for some measurements.

Figure 5 shows visible, thermal, polarization, and the eTherm® color-fused imagery that combines the thermal and polarization information. Two types of crude oil and diesel fuel are apparent in the polarization image, whereas the diesel is slightly less visible in the eTherm image and not at all visible in the visible or thermal images. As expected from the fast tank testing, the thermal contrast is significantly less than that of the polarization. It should be pointed out that the shallow tank and white bottom results in a light-colored blue for the water, making the oil fairly visible. In open ocean conditions, the water color will be much darker and hence reduce the visibility of the oil in the visible imagery.

Results of testing with nonbreaking waves is shown in Figure 6. Again, diesel fuel and two types of crude oil were released into the tank. Although it is not readily apparent in this image, the video shows a slight loss of signal on the back side of the waves in some cases that is not attributable to simple obscuration of the wave. In these cases, the angle is essentially grazing relative to the surface normal of that part of the wave and the signal is consequently reduced. Practically speaking, however, the slight loss of signal is not significant, and it can be said that the detection works in the presence of nonbreaking waves.

Figure 7 shows imagery of two crude oil types mixed together through wave action and in the presence of breaking waves. The foam from the breaking waves shows a higher effective temperature than the surrounding water due to surface roughness and effective emissivity changes. The

FIGURE 4

The moveable bridge over the Ohmsett tank. The Pyxis and visible camera were mounted on the tower at the right end of the bridge. The picture on the right shows the Pyxis and visible camera viewing the tank. Two small spills are visible about halfway down the tank. The wave machine was just started and the waves have almost propagated to the spills. The yellow fast tank is visible on the deck to the right side of the tank.

scale for the polarization image is set so that the foam polarization signature is very close to zero and hence essentially depolarized. However, immediately around the foam, the polarization signatures are strong, and the contrast is unaffected as can be seen in both eTherm and polarization images.

Several attempts were made to assess the limit of sensitivity during this sequence of tests, but the thinnest measureable oil samples tested were 0.5 mm thick. Several opportunities arose to image thinner oil that was in the process of spreading. In one instance, 400 gallons of oil was introduced into the tank, and Pyxis was used to capture imagery as it spread. Based on visual observation and the Bonn appearance chart, thicknesses ranged from sheen through rainbow to metallic and dark. By comparing the measured data to visual observation, the limit of detection appeared to occur around the thick edge of the rainbow sheen. There was no opportunity to physically measure or otherwise characterize the thickness.

FIGURE 5

Visible (upper left), thermal (upper right), DoLP (bottom left), and eTherm fused (bottom right) polarimetric and thermal images of two crude oil types and diesel. The diesel is at the top of the image.

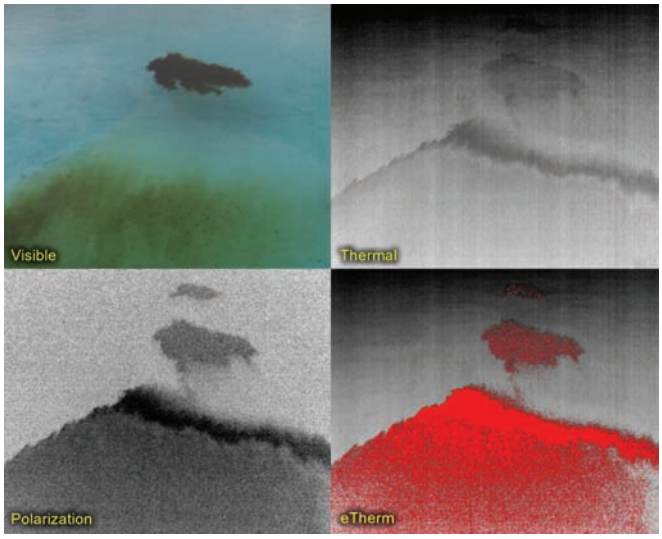

In 2017, ExxonMobil sponsored a second test, and Polaris returned to Ohmsett for further study. In this test sequence, the goal was again to quantify the lower limit of detection, to assess the performance of infrared polarimetry for detection of aged and emulsified oil, to observe the polarimetric signature in the presence of dispersants, and to test the detection approach for oil on sand and rocks.

A 3 × 3 array of 4-foot dividers was set out in the main tank in the first test for minimum detectable thickness. The objective for the array was to control the volume placed in each bin in order to quantify the thickness. Due to the susceptibility for the crude oil to not disperse but to coalesce or clump together in the very small volumes, the thinnest layer to achieve uniform coverage was 125 µm. The other bins contained two control bins with no oil and various thickness ranging between 125 µm and 5 mm. Again, the polarimetric data showed strong detection in every case. However, since it appeared that we still had not reached the limit of detection, we assembled another array with smaller bins in order to more accurately control the volume and to achieve uniform samples. Figure 8 shows the array of bins for this thickness test. In this case, controls with clean water are in the upper left and lower right. For the other four bins, oil was added in increments to give a range of thicknesses. An image was taken for each increment. For the upper middle bin, the first increment was 10 µm, and subsequent additions were also 10 µm. For the upper right bin, the first and subsequent increments were 50 µm. Similar increments were done for the lower left (starting with 250 µm) and lower middle (1.25mm). Therefore,

FIGURE 6

Visible, thermal, polarization, and eTherm images. The two larger spots are two different types of crude oil. The smaller spill visible to the lower right in the polarization images is a 700-ml release of diesel. Thicknesses are estimated to range from 50 µm to 1 mm for the oil. For scale, the white colored deck to the right of the pool is roughly 12 feet wide. The manmade structures around the tank are also polarized. Algorithms such as those producing the red regions in the eTherm image could be exploited for automated detection.

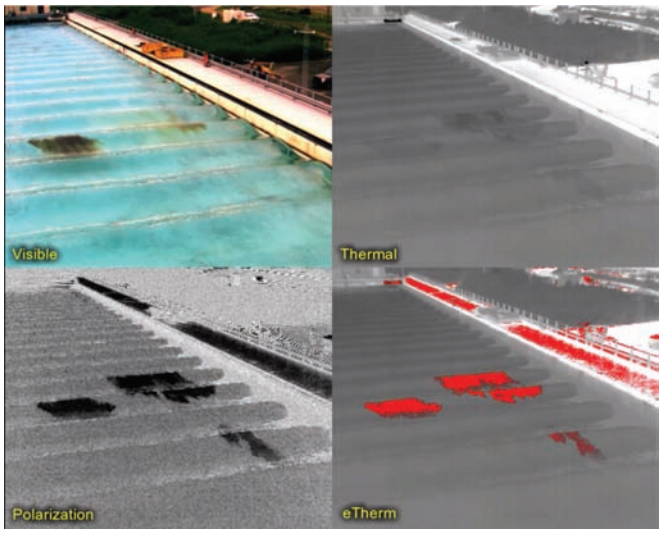

the acquired data sets were as follows: upper middle bin 10 µm, 20 µm, 30 µm, 40 µm, and 50 µm; upper right bin 50 µm, 100 µm, 150 µm, 200 µm, 250 µm; lower left bin 100 µm, 200 µm, 300 µm, 400 µm, 500 µm; lower middle bin 1.25 mm, 2.5 mm, 3.75 mm, 5 mm, 6.25 mm. Figure 8 shows Set 3. Figure 9 shows a plot of the degree of linear polarization (DoLP) for each of the bins as the oil thickness is increased—each bin is one set. The DoLP response shows a peak between 10 and 100 µm with a fall off to an asymptotic response at larger thicknesses. The reason for this peak response results from the relative thickness of the oil and the wavelength of light under these conditions. The conclusion from these data is that the limit of sensitivity lies between 10 and 100 µm, which again corresponds to the metallic thickness of the Bonn scale.

FIGURE 7

Visible, thermal, polarization, and eTherm images in the presence of breaking waves. The signature detected here is a combination of two types crude oil mixed by the wave action. Foam from the breaking waves is white in visible, thermal, and polarization imagery.

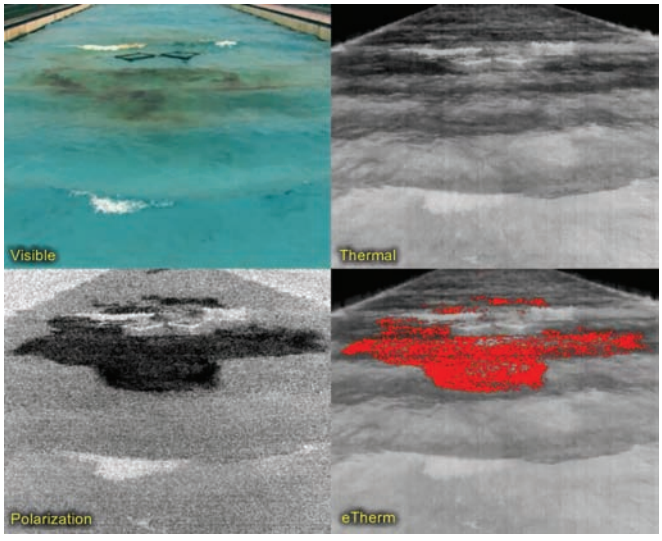

A test for detectability of aged and emulsified oil was also conducted. The Ohmsett staff recommended the following procedure to achieve a realistic emulsion. First, approximately 400 gallons of oil was introduced to the tank and allowed to age over the course of 4 days. After aging, the wave machine was turned on to agitate the oil as it would be in open water. Within a couple of hours, the oil appeared to be fully emulsified with the consistency and color of chocolate pudding. A sample was measured in the lab and established the water content to be 80%. Figure 10 shows one frame from the video that shows strong detection even in the presence of waves. The thermal imagery is confusing due to thermal variations in the waves and the imagery did not consistently show the presence of oil. Although the contrast in the visible is good in the Ohmsett tank, visibility would be significantly less in the open water due to open water being much darker.

A test of oil detection on rocks and sand was also performed. In this case, a beach scenario was assembled from New Jersey beach sand with dark rocks in a containment area. Oil was poured on several of the rocks and on part of the sand. Clean rocks, clean

FIGURE 8

Oil thickness test. Left to right, top to bottom: clean water, 30 µm, 150 µm, 750 µm, 3.75 mm, and clean water.

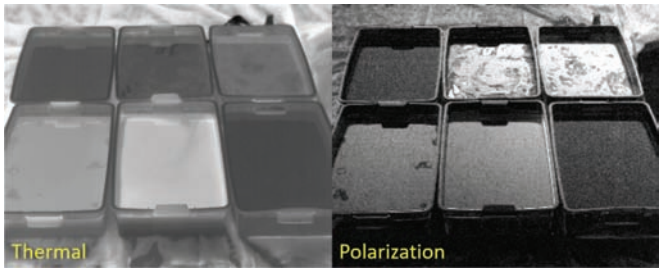

sand, and a bin of clean water were also present as controls. Imagery was first acquired as oil was poured in the sand. Although the oil pooled on the sand, the polarimetric detection was strong and effective. When the oil soaked into the sand and was no longer pooling on top of the sand, the polarization signature disappeared. The oil-soaked rocks showed a strong response in polarization, whereas the thermal imagery of both oiled sand and rocks showed essentially no contrast. Water was then poured onto the oiled sand and rocks to emulate wave action on a beach. When the water floated the oil to the surface of the sand, the polarization once again showed strong detection because the oily water was pooled on the surface of the sand. When the liquid mixture soaked back into the sand, the signature disappeared. The oiled rock retained its detection in polarization.

A final test of the Pyxis infrared polarimetric camera was performed during the application of dispersants. Again, a large quantity of fresh oil was dumped in the Ohmsett tank along with dispersant (Corexit 9500) and with waves present in the tank. The dispersant appeared to be effective by observing the water column as it turned from clear to a murky brown color. There was an initial detection of oil on the surface, but after several waves it was observed that the dispersant was properly breaking down the oil into the water column. Pyxis worked well in that is was able to detect small areas of oil before the dispersant was effective.

Videos of many of the data sets for these tests can be found by searching on YouTube with the search term "Polaris Sensor Ohmsett 2017."

FIGURE 9

Plot of DoLP as a function of oil thickness. The limit of sensitivity for infrared polarimetric detection lies between 10 and 100 µm.

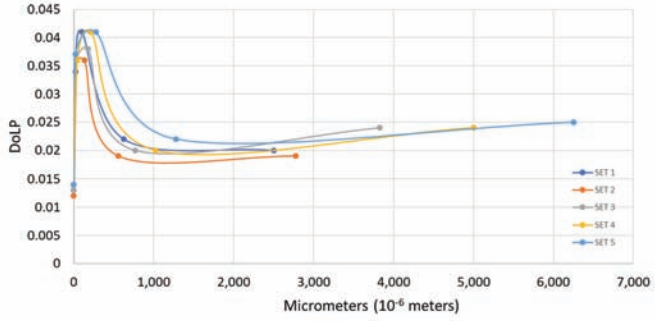

Gulf of Mexico Testing

Polaris participated in two test opportunities in the Gulf of Mexico both near the site of the Taylor Energy Mississippi Canyon 20-A production platform 12 miles south of the mouth of the Mississippi River that was destroyed by Hurricane Ivan in 2004. Although a great deal of remediation has been done, there is still a trickle of oil that can sometimes be seen on the surface of the water near the 440-foot deep well head. The first test was aboard a helicopter that flew over the Taylor Site. Although there were no measurements on the surface to confirm the presence or thickness of oil, visible imagery was acquired simultaneously and observation confirmed wide areas of sheen and much smaller areas of rainbow. Inside the areas of rainbow sheen, metallic could be perceived. Figure 11 shows the visible and eTherm imagery. Many months later, Polaris participated in a cruise to the site on the Marine Spill Response Corporation-operated (MSRC) Oil Spill Response Vessel *Louisiana Responder*. Figure 11 also shows these data, where the thickest oil is inside the boundary of the rainbow sheen, again confirming that Pyxis detects metallic thickness of oil. The airborne data were collected at 400-foot altitude with a depression angle of about 30°, giving a slant range of about 800 feet. In the case of the imagery taken from the ship, the slant range was about 150 feet.

Summary and Future Work

Thermal polarimetric imaging has been demonstrated to be very effective at detecting oil and diesel spills

FIGURE 10

Visible, thermal, polarization, and eTherm images of emulsified crude oil in the presence of waves.

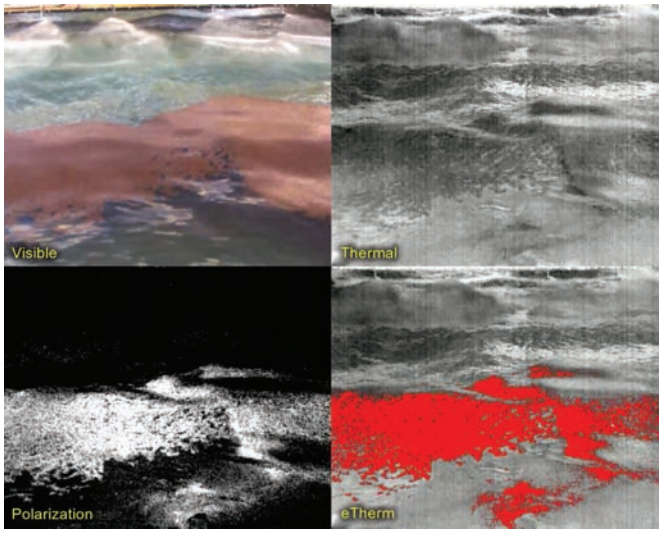

at the Ohmsett test tank under a variety of conditions as well as on two occasions in the Gulf of Mexico. The Pyxis LWIR 640 polarimetric camera was described as well as the phenomenology associated with thermal polarimetric signatures. Pyxis detected oil and diesel on the surface of the water with thicknesses down to 10 µm, in waves, and at times of day in which the thermal signature underwent thermal cross-over. The signatures are strong enough and robust enough in various conditions that there is a strong possibility for automated detection for the oil and gas industry, for environmental monitoring, for ports and harbor surveillance, and other applications.

FIGURE 11

Visible and eTherm images collected in the Gulf of Mexico near the Taylor Energy site. The top set collected from a helicopter at approximately 400-foot altitude. The bottom set collected many months later from MSRC operated Oil Spill Response Vessel *Louisiana Responder*.

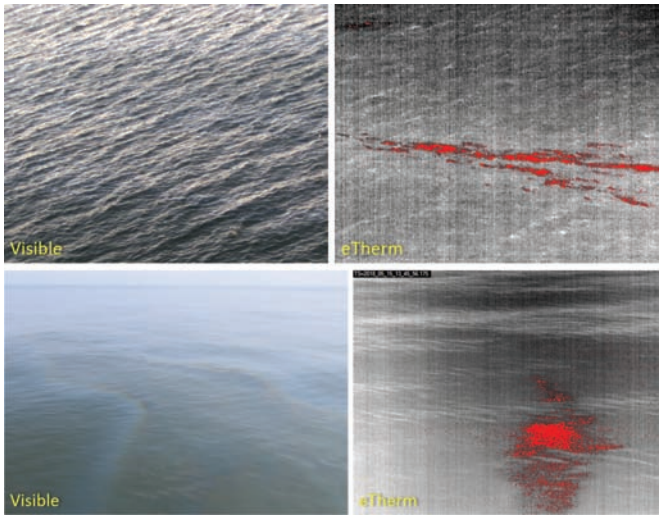

Work will continue to explore oil on water detection through infrared polarimetric imaging through measurement activities as well as through analysis and algorithm development. Further tests, as they are available, will be examined to look at a variety of conditions with as much ground truth as possible for accurate comparisons to conventional imaging techniques. This work will also be leveraged to establish and improve automated detection.

Acknowledgments

This work was funded in part through commercialization efforts under the Small Business Innovative Research program. Polaris testing at Ohmsett was sponsored in part by ExxonMobil Upstream Research Company. We gratefully acknowledge the professionalism, flexibility, and general good nature of the Ohmsett staff over the course of several long days/weeks of testing. Polaris wishes to also gratefully acknowledge the support of MSRC for some of the Gulf of Mexico data collection.

Corresponding Author:

David B. Chenault
Sensor Technologies, Inc.
200 Westside Square, Suite 320
Huntsville, AL 35801
Email: David.Chenault@PolarisSensor.com

References

Allik, T.H., Ramboyong, L., Roberts, M., Walters, M., Soyka, T.J., Dixon, R., & Cho, J. 2016. Enhanced oil spill detection sensors in low-light environments. In: Proc. SPIE 9827, Ocean Sensing and Monitoring VIII. Orlando: SPIE.

Chenault, D.B., Vaden, J.P., Mitchell, D.A., & DeMicco, E.D. 2016. Infrared polarimetric

sensing of oil on water. In: Proc. SPIE 9999, Remote Sensing of the Ocean, Sea Ice, Coastal Waters, and Large Water Regions. Edinburgh, Scotland: SPIE.

Chenault, D.B., & Vaden, J.P. 2018. Infrared polarimetric sensing of oil on water. In: Proc. SPIE 10631, Ocean Sensing and Monitoring X. Orlando FL: SPIE. https://doi.org/10.1117/12.2307032.

Felton, M., Gurton, K.P., Pezzaniti, J.L., Chenault, D.B., & Roth, L.E. 2010a. Comparison of the inversion periods for MidIR and LWIR polarimetric and conventional thermal imagery. In: Proc. SPIE 7672, Polarization: Measurement, Analysis, and Remote Sensing IX. Orlando: SPIE. https://doi.org/10.1117/12.850264.

Felton, M., Gurton, K.P., Pezzaniti, J.L., Chenault, D.B., & Roth, L.E. 2010b. Measured comparison of the crossover periods for mid- and long-wave IR (MWIR and LWIR) polarimetric and conventional thermal imagery. Opt Exp. 18(15):15704-13. https://doi.org/10.1364/OE.18.015704.

Myhr, S., Ax, G., Gill, J., LeClair, L., Sippel, E., Walters, M., & Dixon, R.E. 2018. Mapping and reconnaissance imager, night-enhanced, for sensing of contaminants, oil, and unseen threats (MARINE SCOUT). In: Proc. SPIE 10631, Ocean Sensing and Monitoring X. Orlando: SPIE. https://doi.org/10.1117/12.2303963.

Svejkovsky, J., Hess, M., Muskat, J., Nedwed, T.J., McCall, J., & Garcia, O. 2016. Characterization of surface oil thickness distribution patterns observed during the Deepwater Horizon (MC-252) oil spill with aerial and satellite remote sensing. Mar Pollut Bull. 110(1): 162-76. https://doi.org/10.1016/j.marpolbul.2016.06.066.

Tyo, S., Goldstein, D.H., Chenault, D.B., & Shaw, J.A. 2006. Review of passive imaging polarimetry for remote sensing applications. Appl Opt. 45(22):5453-69. https://doi.org/10.1364/AO.45.005453.